AIAA JOURNAL
Vol. 45, No. 12, December 2007

Technical Notes

TECHNICAL NOTES are short manuscripts describing new developments or important results of a preliminary nature. These Notes should not exceed 2500 words (where a figure or table counts as 200 words). Following informal review by the Editors, they may be published within a few months of the date of receipt. Style requirements are the same as for regular contributions (see inside back cover).

Measurement and Prediction of Noise Propagation from a High-Power Jet Aircraft

Kent L. Gee* and Victor W. Sparrow†
Pennsylvania State University, University Park, Pennsylvania 16802
Michael M. James,‡ J. Micah Downing,§ and Christopher M. Hobbs¶
Wyle Laboratories, Inc., Arlington, Virginia 22202
and
Thomas B. Gabrielson** and Anthony A. Atchley††
Pennsylvania State University, University Park, Pennsylvania 16802

DOI: 10.2514/1.28985

I. Introduction

THE characterization of nonlinear effects in the propagation of high-amplitude jet noise is a topic that has gained renewed interest with the deployment of next-generation fighter aircraft. An amplitude-dependent wave speed, neglected as part of linear acoustics assumptions, results in different portions of a noise waveform traveling at different speeds during propagation. This causes the waveform to steepen and, if nonlinear effects dominate losses, causes acoustic shocks to form. From a frequency-domain standpoint, the waveform steepening results in a transfer of energy from the peak-frequency region in the spectrum primarily upward in the spectrum. Energy transfer downward in the spectrum by nonlinear effects due to the coalescence of shocks is also possible, but the extent to which it impacts high-amplitude jet noise propagation is unknown.

The prediction of high-amplitude noise propagation has been the subject of a number of previous studies [1–3] that have used various forms of the generalized Mendousse–Burgers equation (GMBE)‡‡ to model the propagation. The GMBE is a parabolic nonlinear model equation that accounts for quadratic nonlinearity, geometrical spreading, and absorption and dispersion [4]. Pestorius and Blackstock [1] experimentally and numerically investigated the propagation of finite amplitude noise in a one-dimensional duct. They developed an algorithm that Blackstock [5] later used to propagate an actual T-38 noise recording. Although that study predicted a nonlinear evolution of the jet noise waveform, there was no measurement made at a greater distance to allow a direct comparison of the predicted and actual propagation. Finally, Morfey and Howell [3] and Crighton and Bashforth [2] devised methods by which power spectra could be evolved via an ensemble-averaged version of the GMBE, but both of these methods have fundamental difficulties in that they neglect phase, an essential part of nonlinear propagation physics.

Recently, Gee et al. [6,7] built upon Pestorius and Blackstock's [1] original work and compared the results of numerical propagation of F/A-18E waveforms via their algorithm against measurements that showed evidence of nonlinear propagation [8,9]. Although there were distinct similarities in the high-frequency rolloff trends for comparisons between predicted and measured spectra, there were notable differences as well. These differences were qualitatively confirmed in a similar comparison by Brouwer [10] that employed a different solution technique of the GMBE. Although the reasons for the discrepancies between the nonlinear model and the F/A-18E measurement are still not fully understood, it is believed that environmental and terrain effects significantly contributed to the differences between the experiment and the numerical model, which assumes free-field propagation through a quiescent atmosphere.

The previous F/A-18E comparisons showed the nonlinear model's promise in predicting high-amplitude noise propagation, but known limitations in the experimental setup and measurement environment precluded a more conclusive comparison. Lessons learned from those measurements were incorporated into a test plan for static engine run-up measurements of the F-22 Raptor. Specifically, the Raptor measurements were of greater bandwidth, over a greater propagation range, and the propagation environment was better understood. Relative to the F/A-18E and the prior studies mentioned, this Note represents a considerable development in our understanding of the significance of nonlinear effects in jet noise propagation. After a brief description of the measurement setup, measured and predicted spectra for low- and high-power engine settings are compared and discussed.

II. Measurement Description

The F-22 static engine run-up tests were conducted by Wyle Laboratories and Pennsylvania State University during the early morning on 15 September 2004 at Edwards Air Force Base (EAFB). A measurement array, consisting of Bruel and Kjaer (types 4938, 4939, and 4190) and GRAS (type 40BF) condenser microphones

Presented as Paper 2531 at the 12th AIAA/CEAS Aeroacoustics Conference, Cambridge, MA, 8–10 May 2006; received 22 November 2006; revision received 2 August 2007; accepted for publication 21 August 2007.

*Currently Assistant Professor, Department of Physics and Astronomy, Brigham Young University, N243 Eyring Science Center, Provo, UT 84602; kentgee@byu.
edu. Member AIAA.

†Associate Professor, Graduate Program in Acoustics, 201 Applied Science Building. Senior Member AIAA.

‡Currently Principal Engineer, Blue Ridge Research and Consulting, 13 1/2 West Walnut Street, Asheville, NC 28803. Member AIAA.

§Currently Chief Scientist, Blue Ridge Research and Consulting, 13 1/2 West Walnut Street, Asheville, NC 28803. Member AIAA.

¶Senior Acoustician, 2001 Jefferson Davis Highway, Suite 701. Member AIAA.

**Senior Scientist, Applied Research Laboratory, P.O. Box 30, State College, PA 16804.

††Professor of Acoustics and Chair, Graduate Program in Acoustics, Applied Science Building. Member AIAA.

‡‡This equation is usually referred to in the nonlinear acoustics literature as simply the generalized Burgers equation (GBE).

were located at various distances from 23–305 m along the 125-deg radial (measured relative to the jet inlet.) The microphones were located at a height of approximately 1.8 m. The origin for the measurement array was located approximately 5.5 m (roughly 7–8 jet diameters) downstream from the jet nozzles in an attempt to place the origin near the dominant aeroacoustic source region for high-power engine settings. Note that this is only a rough approximation, because the dominant source region is expected to vary both as a function of frequency and angle. During the tests, the engine farthest from the measurement array was held at idle, whereas the other engine's condition was varied for the run-up tests. Acquisition of the pressure waveforms was carried out using National Instruments 24-bit PXI-4472 DAQ cards with a 96-kHz sampling rate.

The time of the tests was selected to be early morning with the hope of minimizing atmospheric effects that are common during the day at EAFB: namely, a significant temperature lapse and moderate winds. The run-up measurements took place between 0630–0800 hrs Pacific Daylight Time, during which time atmospheric conditions were generally conducive to making propagation measurements. A meteorological station, which consisted of three temperature sensors, two relative humidity sensors, and wind speed and direction gauges, was located 61 m from the aircraft, near the measurement array. The station was used to track the local meteorology near the ground throughout the measurements. The temperature and relative humidity sensors were located at different heights to measure gradients near the ground. The particular measurements highlighted in this Note occurred when there was little or no wind (~0.1 m/s) and small temperature gradients (less than 0.1°C/m) at the tower. For the measurements described in this Note, the ambient pressure, temperature, and relative humidity were 0.92 atm, 14.8°C, and 48%, respectively.

III. Comparison Results

Predicted and measured spectra are presented in this section for two engine conditions, idle and afterburner (AB), which represent the two amplitude extremes of the run-up tests. For both conditions, the nonlinearly predicted spectra were obtained by numerically propagating waveforms recorded at 61 m out to 305 m using the GMBE-based model. Approximately 11 s of data (2^{20} samples) were used in the numerical propagation. The GMBE used in this study incorporates nonlinear effects, spherical spreading, and atmospheric absorption and dispersion. The linear predictions are direct extrapolations of the calculated one-third-octave spectra at 61 m out to 305 m. The extrapolation includes spherical spreading and atmospheric absorption.

A. Idle

The first case to discuss is for both engines at idle. This test represents the lowest overall levels encountered in the run-up measurements and is shown to provide a direct comparison against the AB test. Displayed in Fig. 1 is the comparison between the measured and predicted spectra. Note that there is little difference between the linearly and nonlinearly predicted spectra over the frequency range 20 Hz–4 kHz. Noise-floor limitations preclude a greater analysis bandwidth for the idle measurement. This result indicates that according to the GMBE, the propagation can be considered linear for this case, at least over this frequency range. However, agreement between the predicted spectra and the measured spectra is not particularly good. Below 200 Hz, the measured levels are typically a few decibels greater than predicted. Above 200 Hz, the measured levels are a few decibels less than predicted. A similar discrepancy between the linear model and the measurement is also seen in the AB measurement, shown subsequently, that was made less than 1 min after the idle run. The fact that it is also seen in the low-amplitude idle measurement likely indicates that its causes are linear, rather than nonlinear, propagation phenomena. Particularly, a study [7] of the expected impact of ground reflections over the propagation range and moderately hard ground suggests that the disagreement between the linearly predicted and measured spectral levels between

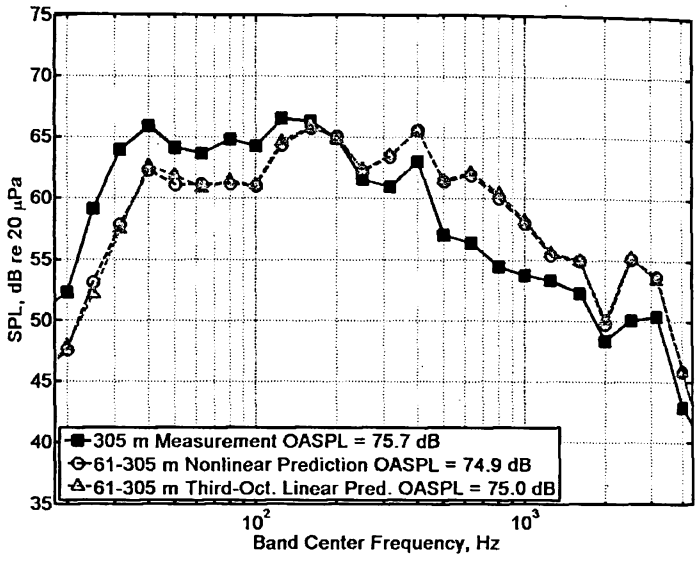

Fig. 1 Comparison between the measured and predicted one-third-octave band spectra for idle at 305 m.

200 Hz and 3 kHz is caused by the variation of ground interference nulls between 61 and 305 m.

B. Afterburner

The comparison between measured and predicted spectra at the highest engine setting, AB, is now discussed. It is noted that both engines were not at high power; rather, only the engine closest to the measurement array was at high power and the other engine remained at idle. Shown in Fig. 2 are the measured and predicted spectra at 305 m and 125 deg for the same frequency range shown for idle. The overall sound pressure level (OASPL) has increased dramatically from idle, by about 45 dB, to a value of nearly 122 dB at 305 m. In Fig. 2, similar differences between the predicted and measured spectra as discussed for idle are evident below 200 Hz. Above about 2 kHz, the nonlinearly predicted spectrum more closely matches the measured spectrum at these higher frequencies, with an average reduction of approximately 4 dB per octave, which is very close to the 3 dB/octave expected for a shock-dominated waveform. However, the linearly predicted spectrum has a sharper rolloff, which results from increased atmospheric absorption at high frequencies. The difference between the linear and measured spectra grows to about 8 dB at 4 kHz. This greater rolloff for the linear spectrum at higher frequencies is better shown in Fig. 3, which provides an expanded frequency range for the AB comparison. This figure more clearly reveals the high-frequency difference between the linearly

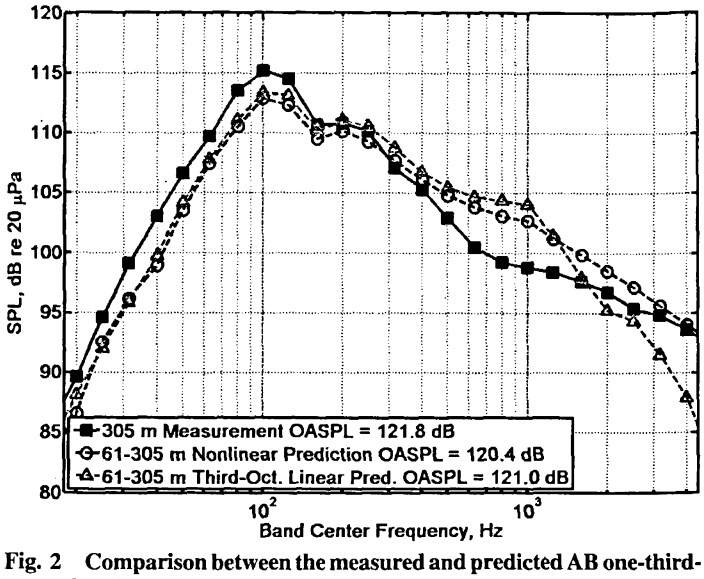

Fig. 2 Comparison between the measured and predicted AB one-third-octave band spectra at 305 m. The maximum third-octave band shown is 4 kHz to directly compare with the idle measurement at high frequencies.

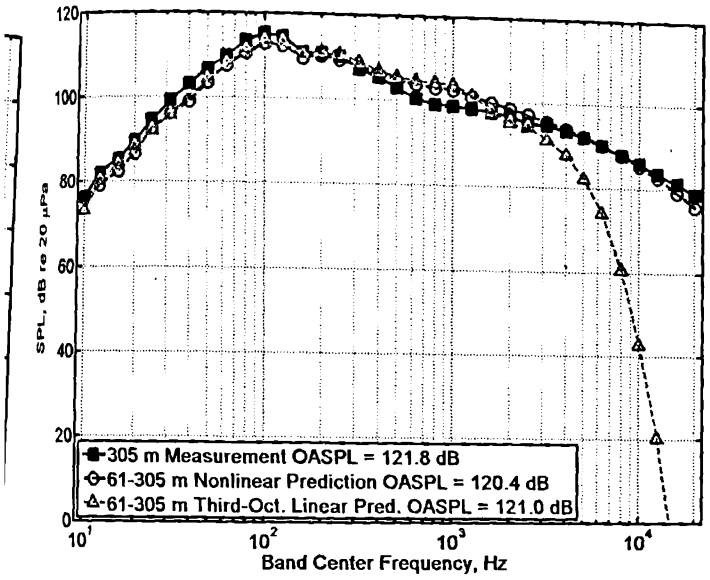

Fig. 3 Comparison of measured and predicted spectra for the AB case in Fig. 2. The frequency range was extended in this plot from 10 Hz to 20 kHz to show the extreme differences between the measurement and linear prediction at high frequencies.

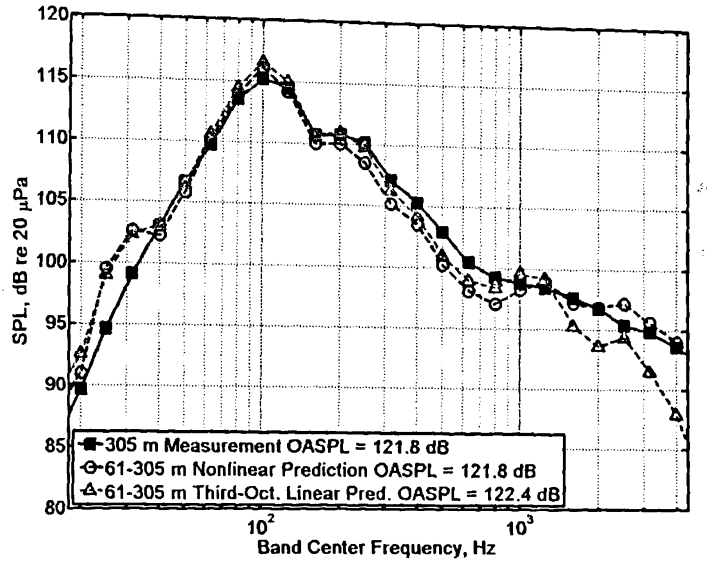

Fig. 4 Improved agreement between the AB nonlinearly predicted and measured spectra from Fig. 2 after empirically correcting the predicted spectra. See Sec. III.C for a discussion of how the correction was applied.

predicted and measured spectrum that grows to nearly 140 dB at 20 kHz. On the other hand, the spectrum calculated from the nonlinearly propagation model only differs from the measured spectrum by about 3 dB at 20 kHz. The high level of agreement between the GMBE-based propagation model and the measured spectrum is strong evidence that the lack of high-frequency absorption in the measured propagation is due to nonlinear effects. Furthermore, the slopes of the nonlinearly predicted and measured spectra indicate the presence of acoustic shocks in the waveform.

C. Further Discussion

Two other points merit discussion. The first is the apparently negligible impact that nonlinearity has on the OASPL calculation for this case. As is seen in the legend for Fig. 3, the linearly and nonlinearly predicted OASPLs differ by only 0.6 dB, which is not significant. This finding is different from the previous F/A-18E comparisons, for which the nonlinearly predicted OASPL was about 4 dB less than linearly predicted over an 18–150-m range [6]. A possible cause for the difference is that the F/A-18E OASPL near the source was significantly greater (150 dB re 20 μPa at 18 m), which may have resulted in a greater impact of nonlinearity on overall levels. However, the different propagation ranges may also play a role. Research is being conducted to better understand the impact of nonlinear propagation on single-number metric calculations (e.g., *A*-weighting) and on actual human perception (for example, see [11]).

Second, the similarity of the propagation environment effects between the idle and AB comparisons below 2 kHz also suggests a means by which the low- to midfrequency agreement between the measurement and nonlinear predictions in Figs. 2 and 3 may be empirically improved. This is carried out by using the idle measurement to calculate the difference between the real atmospheric propagation and the assumed free-field propagation through a quiescent homogeneous atmosphere from 61–305 m. This effect, calculated in decibels for the one-third-octave bands below 2 kHz, is then added to the AB nonlinearly and linearly predicted spectra. Recall that the AB data were collected less than 1 min after the idle data and that atmospheric conditions were fairly constant. It is noted that this approach assumes that the effects not accounted for in the prediction models (e.g., ground reflections, refraction, turbulence, etc.) impact the high- and the low-amplitude propagation exactly the same way. Although this may be shown not to be strictly true, the small differences between the free-field linear and nonlinear predictions below 2 kHz in Fig. 2 demonstrate that nonlinearity is projected to have little effect on the spectra below 2 kHz for this propagation range. Consequently, addition of the idle-measured phenomena to the predicted spectra at 305 m for AB does generally improve agreement between the measured and nonlinearly predicted spectra, as can be seen in Fig. 4. The increased error below 40 Hz could be related to the fact that the idle measurement has a higher percentage of its power below 40 Hz compared with the AB measurement.

IV. Conclusions

These comparisons of F-22 run-up measurements against the predictions of a generalized Mendousse–Burgers equation-based numerical model show clearly what previous studies have not shown. For both engines at idle, there is little difference between nonlinear and linear predictions, and the results of the models match the measured spectrum within a few decibels up to 4 kHz. Because of the low acoustic amplitudes present in the idle measurement, any differences between the predictions and the measured spectrum are attributed to the outdoor propagation environment. For one engine at afterburner, there is a significant excess of high-frequency energy in the 305-m measurements relative to a linear propagation prediction. This excess is closely predicted by the nonlinear propagation model, demonstrating that the noise propagation from high-power military jet aircraft can be significantly nonlinear.

Acknowledgments

K. L. Gee, V. W. Sparrow, M. M. James, J. M. Downing, and C. M. Hobbs were supported by the Strategic Environmental Research and Development Program. T. B. Gabrielson and A. A. Atchley acknowledge the support of the Office of Naval Research.

References

[1] Pestorius, F. M., and Blackstock, D. T., "Propagation of finite Amplitude Noise," *Finite Amplitude Wave Effects in Fluids*, edited by L. Bjorno, IPC Business Press, Surrey, England, U.K., 1973, pp. 24–29.

[2] Crighton, D. G., and Bashforth, S., "Nonlinear Propagation of Broadband Jet Noise," AIAA Paper 80-1039, June 1980.

[3] Morfey, C. L., and Howell, G. P., "Nonlinear Propagation of Aircraft Noise in the Atmosphere," *AIAA Journal*, Vol. 19, No. 8, 1981, pp. 986–992.

[4] Hamilton, M. F., and Morfey, C. L., "Model Equations," in *Nonlinear Acoustics*, edited by M. F. Hamilton and D. T. Blackstock, Academic, San Diego, CA, 1998, Chap. 3, pp. 41–63.

[5] Blackstock, D. T., "Nonlinear Propagation Distortion of Jet Noise," *Proceedings of the Third Interagency Symposium on University Research in Transportation Noise*, edited by G. Banerian and P. Kickinson, Univ. of Utah, Provo, UT, 1975, pp. 389–397.

[6] Gee, K. L., Sparrow, V. W., Gabrielson, T. B., and Atchley, A. A., "Nonlinear Modeling of F/A-18E Noise Propagation," AIAA Paper 2005-3089, May 2005.

[7] Gee, K. L., "Prediction of Nonlinear Jet Noise Propagation," Ph.D. Thesis, Graduate Program in Acoustics, Pennsylvania State Univ., University Park, PA, 2005.

[8] Gee, K. L., Gabrielson, T. B., Atchley, A. A., and Sparrow, V. W., "Preliminary Analysis of Nonlinearity in F/A-18E/F Noise Propagation," *AIAA Journal*, Vol. 43, No. 6, 2005, pp. 1398–1401.
[9] Gee, K. L., Atchley, A. A., Falco, L. E., Gabrielson, T. B., and Sparrow, V. W., "Bispectral Analysis of High-Amplitude Jet Noise," 11th AIAA/CEAS Aeroacoustics Conference, Monterey, CA, AIAA Paper 2005-2937, May 2005.
[10] Brouwer, H. H., "Numerical Simulation of Nonlinear Jet Noise Propagation," AIAA Paper 2005-3088, May 2005.
[11] Gee, K. L., Swift, S. H., Sparrow, V. W., Plotkin, K. J., and Downing, J. M., "On the Potential Limitations of Conventional Sound Metrics in Quantifying Perception of Nonlinearly Propagated Noise," *Journal of the Acoustical Society of America*, Vol. 121, No. 1, 2007, pp. EL1–EL7. doi:10.1121/1.2401193

C. Bailly
Associate Editor

Thermal Choke of the Evaporation Wave During Laser Ablation

Zhaoyan Zhang* and Biqing Sheng†
University of Nebraska–Lincoln, Lincoln, Nebraska 68588

DOI: 10.2514/1.34050

Nomenclature

c_p	=	specific heat
h	=	specific enthalpy
h_{fg}	=	latent heat of evaporation
M	=	Mach number
p	=	pressure
q	=	heat addition
R	=	gas constant
s	=	entropy
T	=	temperature
v	=	velocity
z	=	compressibility factor
γ	=	ratio of specific heats
ρ	=	density

Subscripts

s	=	value at the stagnation point
0	=	value for the excited solid phase
1	=	value for the gaseous phase

Superscripts

*	=	value at the sonic point

Introduction

LASER ablation has a wide range of applications in engineering and scientific research. The laser ablation process during short-pulsed laser operation consists of three coupled processes: 1) heat conduction within the solid, 2) flow through a discontinuity layer attached to the solid surface, and 3) shock wave expansion of the laser-induced vapor/plasma. Tremendous research efforts have been directed toward understanding of the laser ablation process. Krokhin [1] was the first to formulate the physical mechanism of evaporation coupled with expansion of vapor and plasma. He postulated that the vapor leaving the evaporation wave is of sonic speed. Anisimov [2] and Knight [3] independently proved that the velocity of the vapor leaving the evaporation wave cannot exceed the speed of sound. Von Allmen [4] summarized the governing equations for the evaporation wave and presented two formulations. In the first formulation, the conservation equations together with the state equation form a well-posed problem. In the second formulation, the conservation equations together with the speed of sound form a well-posed problem. No attempt has been made to reconcile the ambiguity. Kelly and Braren [5] investigated the effects of the Knudsen layer on laser ablation. They suggested that the flow leaving the evaporation wave is approximately of sonic speed.

The previous studies either concluded or postulated that the velocity of vapor leaving the evaporation wave is limited by the speed of sound. However, the mechanism of the evolution of the evaporation wave during laser ablation remains unclear. In the present Note, the flow through the discontinuity layer attached to the solid surface is studied based on a compressible flow framework. The evaporation wave behaviors under different conditions are discussed.

The formulation of the physical mechanism of evaporation coupled with vapor expansion follows that of Krokhin [1]. During the laser ablation of materials, the laser energy is absorbed within a short penetration depth of the material. This leads to an increase of the surface temperature. A transient one-dimensional model can be used to describe the heat diffusion process within the solid. When the temperature of the material becomes sufficiently high, evaporation of the material occurs. At high laser intensity, the surface temperature is superheated to a temperature far beyond the saturation temperature to support the finite rate of evaporation. At this stage, the thermal diffusion stops playing a significant role. Without loss of generality, single-step evaporation from solid to vapor is assumed. The high-temperature solid expands into a rarefaction wave and experiences a phase change to vapor. The schematic of the evaporation wave is shown in Fig. 1. The solid surface recedes at velocity v_0 during laser ablation. The evaporation wave appears to be unsteady. A coordinate transformation can be done by attaching the moving evaporation wave to the receding solid surface. This simplifies the conservation equations across the evaporation wave, which can be expressed as

$$\rho_0 v_0 = \rho_1 v_1 \tag{1}$$

$$p_0 + \rho_0 v_0 v_0 = p_1 + \rho_0 v_0 v_1 \tag{2}$$

$$h_0 + \frac{v_0^2}{2} = h_1 + \frac{v_1^2}{2} \tag{3}$$

where ρ is the density, v is the velocity, p is the pressure, and h is the specific enthalpy. The subscript 0 indicates values for the superheated solid phase, and the subscript 1 indicates values for the gaseous phase. Because of the large difference between the density of solid and vapor, the velocity of vapor is much larger than the velocity of solid ($v_1 \gg v_0$). The $v_1 + v_0$ on the right-hand side of the conservation equations is reduced to v_1. This simplification has been commonly used by previous researchers [1]. The vapor generated then expands into a shock wave. The expansion process of the laser-induced vapor/plasma can be expressed by Euler equations. A detailed formulation of the laser ablation can also be found in Zhang et al. [6].

The evaporation wave is a finite rarefaction wave in nature, in which the pressure and density decrease as the velocity increases. It is well known that a finite adiabatic rarefaction wave experiences a decrease in entropy and thus is impossible to occur. This dictates that the evaporation wave be a finite rarefaction wave subject to heat addition, which is due to the difference between specific heats of solid and vapor and the latent heat of evaporation. The enthalpies of the solid and vapor can be expressed as

Presented as Paper 2579 at the 37th AIAA Thermophysics Conference, Portland, OR, 28 June–1 July 2004; received 15 August 2007; accepted for publication 24 August 2007.

*Assistant Professor, Department of Mechanical Engineering.
†Graduate Research Assistant, Department of Mechanical Engineering.